NANO LETTERS

2005
Vol. 5, No. 12
2605−2612

Interaction of Polyelectrolytes and Their Composites with Living Cells

Munish Chanana,[†,‡,§] Alessandra Gliozzi,[†] Alberto Diaspro,[†] Irina Chodnevskaja,[||] Sabine Huewel,[‡] Vasiliy Moskalenko,[||] Karin Ulrichs,[||] Hans-Joachim Galla,[‡] and Silke Krol*[,†]

CNR-INFM, Department of Physics, University of Genoa, 16146 Genoa, Italy, Department of Biochemistry, Westfälische Wilhelms-University of Münster, D-48149 Münster, Germany, and University of Würzburg Hospital, Department of Surgery, Experimental Transplantation Immunology, Oberdürrbacher Strasse 6, D-97080 Würzburg, Germany

Received October 27, 2005; Revised Manuscript Received November 14, 2005

ABSTRACT

Since the layer-wise polyelectrolyte deposition offers the opportunity to modify surfaces for biomedical applications, interactions and toxicity between polyelectrolytes and living cells become interesting. The aim of the present work is to determine the different factors such as contact area, charge, and transplantation site that influence the cell reaction to a specific polymer. We found that toxicity is influenced by all these factors and cannot be tested easily in a model.

Since the 1980s when the microencapsulation of living cells, like for example pancreatic islets[1] or hepatocytes,[2] became a promising application in transplantation medicine, the field of polymer-based therapies in medicine has exploded. More and more researchers embedded cells or cell aggregates, for example, in alginate beads.[3−7] But not only has the coating of living cells shown promise, also the linkage of drugs to polymers as carriers was exploited.[8,9]

Progress in recent years in this field was amazing, and also new methods were developed like the layer-by-layer technique[10,11] for the deposition of highly charged polyelectrolytes in an organized manner onto charged surfaces, e.g., living cells.[12,13] A serious obstacle is cytotoxicity of polyelectrolytes or of their metabolic products after degradation. Studying the literature carefully gives evidence that cytotoxicity depends on the polyions' functional groups. But it became also very clear that there is a strong difference in toxicity if the polymer enters the cell[14] or is only in contact with the membrane.[15] So the very same polyelectrolyte can induce immediate cell death or enhance the adhesion of the cells to surfaces. Furthermore, the investigations of de Rosa et al.[15] gave evidence that the surface charge also plays a crucial role in cell survival and adhesion of cells.

This somehow surprising discrepancy in toxicity was the starting point for our present study. We investigated the influence of contact area and polyelectrolyte charge with living cells from different tissues. The first set of experiments focuses on the interactions of different polyelectrolyte application forms with a confluent layer of a primary culture of PBCEC (*porcine brain capillary endothelial cells*) as in vitro model of the blood−brain barrier. The polyions were exposed as solution and as coating on nanoparticles or microparticles to the cells. The change in their tight junction integrity was measured by means of impedance of the cell layer. In a second set of experiments the polyions as coating for alginate particles were implanted in different tissues in Lewis rats in order to study the immune response. After 3 weeks in the rat, the fibrotic overgrowth and revascularization of the implanted material were assayed and served as a rough estimation for the biocompatibility of the tested polyelectrolyte. The results of both studies show clearly that a general statement about the cytotoxicity of polyelectrolytes cannot be made.

The polyelectrolytes as solution were exposed to a confluent layer of PBCEC on a filter or a gold electrode to perform TEER (transendothelial electric resistance) or electric cell−substrate impedance sensing (ECIS) measurements. Both types of measurements give information about the resistance of the confluent cell. In the case of cell damage or disconnection of the tight junctions of the PBCE cells, an increase in the impedance or a decrease in the resistance to the applied electric field could be observed. The time in which the effect is observable gives evidence of the degree of cell damage.

For TEER, the medium was partly exchanged to the polyelectrolyte solution or polyion-coated particle suspension

* Corresponding author: e-mail, krol@fisica.unige.it.
[†] University of Genoa.
[‡] Westfälische Wilhelms-University of Münster.
[§] Present address: MPI for Colloids and Interfaces, D-14424 Potsdam, Germany.
[||] University of Würzburg Hospital.

10.1021/nl0521219 CCC: $30.25
Published on Web 11/24/2005

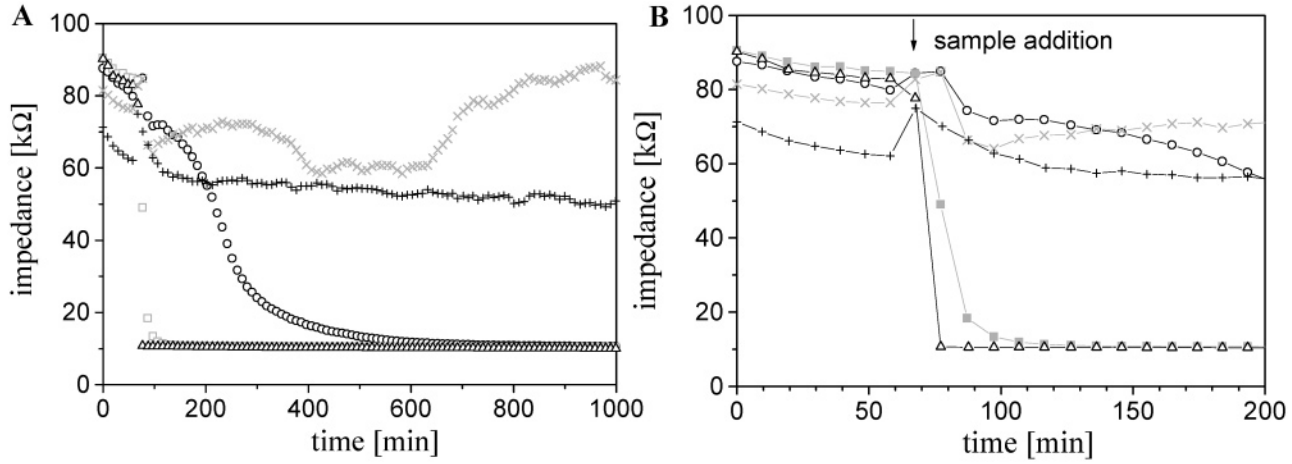

Figure 1. ECIS measurement, impedance vs exposition time for PBCEC layer measured with 100 Hz: (○) PSS; (□) PDADMAC; (△) PAH; (+) control without exchange of the medium; (×) control with exchange of the medium. The cells were exposed to different polyelectrolyte solutions (2 mg/mL). (A) The complete time scale of 1000 min. (B) The time scale only of the first 200 min. The line should only guide the eye.

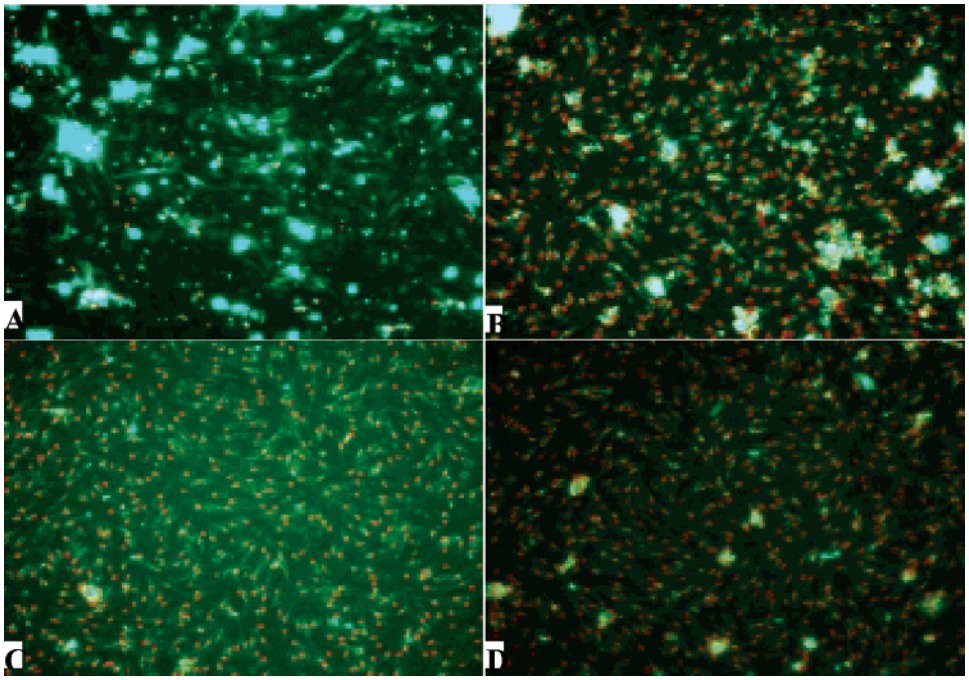

Figure 2. Fluorescence micrograph of the PBCEC after treatment with different concentrations of PAH (B−D). The bright green fluorescence of calcein indicates living cells while the red staining of the nucleus by means of ethidium homodimer occurs only in late apoptotic or dead cells. (A) Confluent monolayer of living cells before polyelectrolyte treatment. (B) After 10 min of incubation in the presence of 50 μL of PAH solution. (C) After 10 min of incubation in the presence of 100 μL of PAH solution. (D) After 10 min of incubation in the presence of 200 μL of PAH solution.

in the upper filter compartment. For ECIS, the growth medium was doped with the particle or polyelectrolyte solution. Then the resistance or impedance of the cell layer was detected with time. In Figure 1 the impedance of the cell layer against time is depicted.

After an equilibration time of 60 min, the polycations were injected directly in the upper filter compartment. From the diagram in Figure 1B it can be seen that for polyallylamine hydrochloride (PAH) the impedance value diminishes within 5 min from initially 95 kΩ to a final value of 10 kΩ. The impedance after addition of the polydiallyldimethylammonium chloride (PDADMAC) solution reaches the same value within 40 min. The results are more promising for the tested polyanion polystyrenesulfonate (PSS) sodium salt. In that case the impedance decreased to the final value only after 800 min. But for both controls, with and without medium change, a slight diminution of the impedance was observable. From these results we assume that positive charges damage the cell layer more than negative ones. But it has to be taken into account that the charge density in the added solutions is not equal for each polyelectrolyte solution. The PAH solution contains two times more positive charge than the PDADMAC solution and 10 times less charge than the negatively charged PSS.

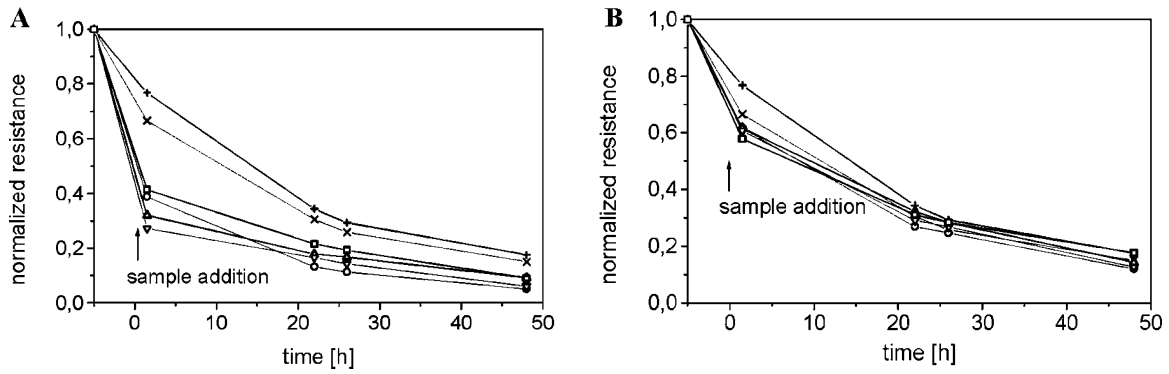

Figure 3. TEER measurement, normalized resistance vs exposition time for PBCEC layer with $CaCO_3$ crystal differently prepared: (○) PSS; (□) PDADMAC; (△) PAH; (▽) PAH in pure H_2O; (+) control without exchange of the medium; (×) control with exchange of the medium. If not indicated otherwise the preparations were all carried out in 0.5 M NaCl solution. The lines should guide the eye. (A) 1:10 dilution and (B) 1:100 dilution of $CaCO_3$ crystal suspension.

To study the influence of the charge density on the cytotoxicity and to get a clearer idea of the nature of the cell damage (cell death or loosening of the tight junctions), we varied the polyelectrolyte concentration and measured the amount of dead cells. The cytotoxicity test in our case based on the addition of different volumes of PAH solution to the cell layer and a live/dead staining by means of calcein AM and ethidium homodimer. Dead or late apoptotic cells appear red in the fluorescence microscopy while the calcein is metabolized and fluoresces bright green.

It becomes obvious from the live/dead staining depicted in Figure 2 that for all three tested PAH concentrations the cells were mainly (>95%) dead (Figure 2B−D) while for the untreated cell layer only an <5% dead or apoptotic cells were counted. From this observation we assume that the decrease in the ECIS measurements is due to cell death and not induced by disconnection of tight junctions. Furthermore it can be concluded that the cytotoxic effect is not concentration dependent in the tested concentration range.

While the application of a polyelectrolyte solution to the cell layer leads to contact on the complete cell surface, polyion-coated particles of different size interact only with parts of the cell surface. To clarify the influence of the contact area two kinds of particles, $CaCO_3$ crystals and nanogold were used. Both cores were chosen because they are generally well tolerated by cells and remain inside the capsule. Treatment of cells in accordance to the experiment described for the PAH solution with uncoated calcium carbonate crystals showed only a slightly increased number (5−10%) of dead cells (data not shown).

Figure 3 shows two diagrams of the TEER versus the time for coated $CaCO_3$ crystals with PAH, PSS, and PDADMAC as outermost layer. For the $CaCO_3$ experiments, we performed also ECIS measurements, but the results were mainly consistent with those by TEER (data not shown).

However, the cells were exposed to two dilutions of the coated crystal suspension to observe a possible concentration effect. The values were normalized to the initial resistance. From the control experiment with medium change, it can be stated that changes in the conditions generally induce a decrease in the resistance of around 10%. Addition of polyion-coated crystals in a 1:10 dilution (Figure 3A) induces some effect on the cell resistance, while the 1:100 dilution (Figure 3B) showed no significant decrease in comparison to the control with medium change. Again PAH-finishing crystals give the strongest diminution of the resistance while that for PDADMAC was the lowest, but generally all the values are close together. From the result for PAH in pure water instead of 0.5 M NaCl, it can be concluded that the charge density plays a role.

To reduce the particle size in the next set of experiments, the cell culture medium was supplemented with polyelectrolyte-coated nanogold. These nanogold particles were coated with two to five polyelectrolyte layers.

Figure 4 shows the ECIS measurement for PBCEC treated with polyelectrolyte-coated nanogold. Noteworthy is that also the number of applied layers plays a role and not only the surface charge. In both cases the impedance decrease is more prominent with the lower number of layers and the results support the previous observations that the PAH is much more toxic than PSS. Especially for five layers the diminution for PSS as the last layer is comparable to that for untreated control cells. Anyhow, from the experiments with different polyion applications it can be stated that the positive polyelectrolytes have a stronger impact on the cell system than the negative ones and the primary amine group of the PAH is more toxic than the ammonium function of PDADMAC (Table 1).

Goodman et al.[16] found that nanogold functionalized with positive side chains (quaternary ammonium group) have a moderate cytotoxic effect on Cos-1 cells, red blood cells, or bacteria cultures (*Escherichia coli*) while negatively charged side chains (carboxylate group) are nontoxic. This is in good agreement with our findings for the positive and negative charged outermost layer on nanogold (Figure 4) and demonstrates that quaternary ammonium groups show a slightly lower cytotoxicity (Figures 1 and 3). The decrease in response of the cells from a polyelectrolyte solution to polyions assembled in layers with counterions implies that only free charges damage the cell walls and induce apoptosis (Figures 1 and 2).

The influence of the particle size is described in the literature contradictorily and only little is known about this aspect. Yin and co-workers[17] found no significant difference in the cytotoxicity of 10 or 150 nm nickel ferrite particles

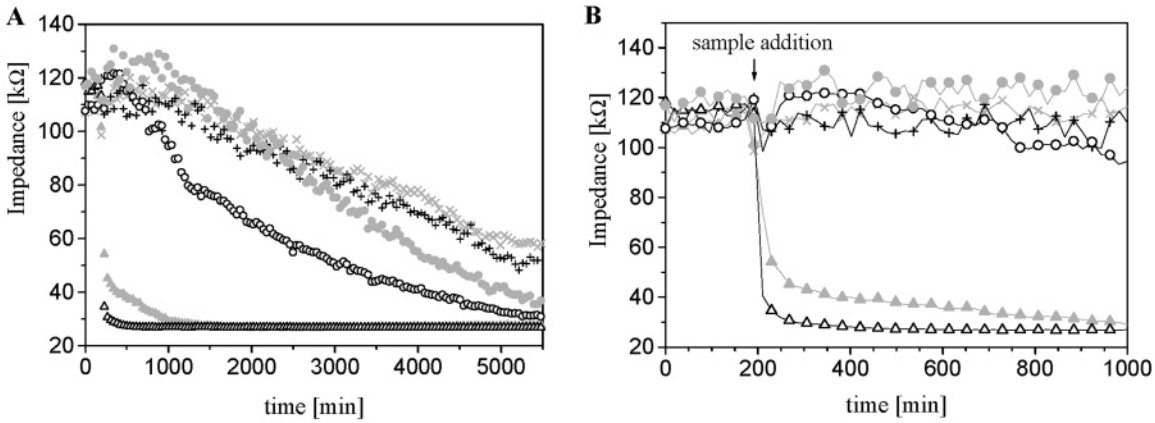

Figure 4. ECIS measurement, impedance vs exposition time for PBCEC layer measured with 100 Hz: (△) two layer, PAH; (○) three layer, PSS; (▲) four layer, PAH; (●) five layer, PSS; (+) control without exchange of the medium; (×) control with exchange of the medium. Cells were exposed to nanogold coated with different numbers of layers and polyelectrolytes. (A) Complete time scale of 5500 min. (B) Time scale of the first 1000 min. The line only should guide the eye.

Table 1. Overview of the Results for Different Polyelectrolyte Preparations and Particle Sizes

polyelectrolyte application	cytotoxic effect	time to reach final value (min)
PE solution		
PAH	strong	5
PDADMAC	strong	40
PSS	medium	800
coated crystal (5−7 μm)		
$CaCO_3$	low	~1200
PAH finishing	medium	~1200
PDADMAC finishing	low	~1200
PSS finishing	low	~1200
coated nanogold (15−18 nm)		
PAH, two layers	strong	250
PAH, four layers	strong	1000
PSS, three layers	low	5000
PSS, five layers	low	>5500

for Neuro-2A cells. Only in the case where one or two layers of oleic acid are applied are the bigger particles more toxic than the smaller ones. Another study by Liu et al.[18] focused on the toxicity of different sizes of fly ash particles on rat alveolar macrophages. The particle sizes varied between 10 μm and several hundred nanometers. They proved that the cytotoxicity of the minuscule particles is augmented in comparison to the larger ones. Also Rodrigo et al.[19] found a stronger influence of the smaller polyethylene particles (<30 μm) on human osteoblastic cells. In their case, this effect was desired.

In the presented study, the cytotoxicity of the coated nanoparticles (15 nm) is higher than that of the microparticles (5−10 μm). We assume that the increased toxicity of the nanogold particle in comparison to the bigger calcium carbonate particles is due to a partial particle uptake in the case of nanometer size while the microparticles only interact peripherally with the cell membrane. The interaction between free charges on the microcapsule surface with counterions in the cell membrane leads to disturbance of the cell and slight apoptosis. But uptake of nanoparticles can interfere in a more severe way with the cells and hence induces more damage. Moreover the uptake of positively charged particles can be facilitated because it was shown that, e.g., the cationization of BSA improves the delivery to the brain via vector-mediated transcytosis through the blood−brain barrier.[20] But it still lacks the evidence, for example, that nanogold particles can be found in the basolateral compartment of the experimental setup. Future studies will focus on this issue.

From the former experiments it became clear that the particle size is of importance for the polyelectrolyte cytotoxicity to the same cell type but for possible implantation of the material in the body also the response of the host tissue is interesting. In that case not only one cell type is involved in a response but also numerous different mechanisms such as the direct contact to the environmental cells, recognition by macrophages, or connection to the blood stream must be taken into account. To get a deeper insight in the immune response to the polyelectrolyte material, no model is complex enough. So we implanted templates coated with the polyelectrolytes in different positions in an animal model. Alginate beads were used because they are well described as immune protection for pancreatic islets transplantation. Furthermore they are big enough to allow a recovery of the beads after several weeks in the body. For a rating of the biocompatibility of an unknown material in contact with tissue, two factors are crucial: the revascularization of the graft which allows a connection to the recipient's blood circuit and the fibrotic overgrowth of the implant/transplant which inhibits the exchange with the environment and can finally lead to apoptosis or necrosis of the microencapsulated cells.

Finally our observations for the nanogold with different numbers of layers confirm the findings of Zhu et al.[21] who stated an improved biocompatibility for human endothelia cells with chitosan as outermost layer. They found better results, i.e., better shape of the attached cells, for a higher number of layers. This is in good accordance to our observations for encapsulated nanogold that shows a higher potential to damage the endothelia cells of the blood−brain barrier with only two or three layers (Figure 4). The

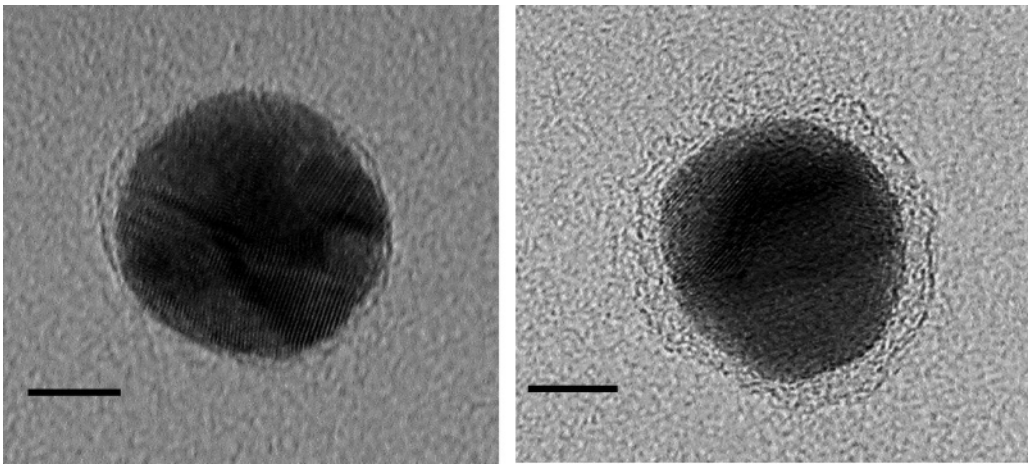

Figure 5. TEM images of nanogold particles with (A) PAH/PSS and (B) $(PAH/PSS)_2$ coatings. The scale bars in both images indicate 5 nm.

assumption that this is due to incomplete coverage is approved by the inhomogeneous thickness of the deposited two layers (Figure 5A) onto the nanogold. The thickness is nearly uniform if four layers were applied (Figure 5B).

Apart from the direct cytotoxicity, the immune response to charge surface is more complex. So the interaction between environmental tissue and polymer coating can only be investigated in the body. To gain results for later immune-protected transplantation, we choose as implantation site for polyelectrolyte-coated alginate beads the kidney capsule and the peritoneum near the liver. For reasons of comparison and due to the fact that immune response is somehow individual, we implanted uncoated alginate beads as well. They remained in the animal for 3 weeks, and then the immune response was evaluated in terms of fibrosis and neovascularization. The evaluation was carried out by appraising photographs of the implantation site as well as a histological determination of the tissue slices. The histology was performed by a Masson−Goldner staining which stains the collagen in the connective tissue of the fibrotic capsule blue. In Figure 6 the surgery pictures (A−C) and the Masson−Goldner staining of the fibrotic capsule (D−F) illustrate the tissues 3 weeks after implantation.

In Figure 6A the right kidney was imaged where the neat alginate beads have been injected underneath the kidney capsule. The picture shows a low fibrotic overgrowth of the alginate beads, so the single particles are distinguishable and the translucent appearance is still clearly observable. But only a few new blood vessels have appeared.

The situation changes if the capsules are coated with PAH/PSS/PAH, finishing with a positive surface charge (Figure 6B). These beads were implanted in the left kidney of the same rat. In that case the particles are nearly completely covered with a whitish material, the fibrotic capsule. Also the revascularization of the region differs. In case of the neat alginate only one single blood vessel (Figure 6A) can be found, while with the positive polyelectrolyte as last layer a network of new vessels all over the surface is detectable. But comparison of the Masson−Goldner staining of kidney slices of the regions in contact to the alginate beads reveals that the collagen-containing fibrotic capsule is in both cases nearly equally thick (blue regions in parts D and E of Figure 6). In higher magnification one could see as well that collagen organization in the fibrotic capsule in case of PAH/PSS/PAH coating is less dense in comparison to the uncoated alginate beads (data not shown).

The most interesting result was gained with the PAH/PSS/PAH coated particles in the peritoneum (Figure 6C). Here, the fibrotic overgrow is minimal, the beads are distinguishable and also the transparence of the material can be observed. This observation from the surgery pictures is supported by the Masson−Goldner staining which did not show any blue-stained regions in the tissue slice (Figure 6F). Moreover the beads are embedded in a tight network of capillaries. This effect is most desirable because in that way an exchange between blood and the products from the cells trapped inside the beads is enhanced.

In general it is known that fibrosis leads to the regression of blood vessels of a region.[22] Hence, an augmented growth of blood vessels in a fibrotic capsule like the one shown in Figure 6B is somehow surprising. A possible explanation is that the positive surface charge of the coated particles attracts fibroblasts or macrophages as well as enhances the neoangiogenesis. This is in agreement with the results of de Rosa et al.[15] and others[23,24] who found that the surface charge influences the cell behavior and positive charges are cell adhesive while uncharged or negatively charged surfaces are nonadhesive for cell, and this can induce extended fibrosis. In the context of the results with the alginate beads, it is interesting to mention the finding of Elbert et al.[24] who created a nonadhesive surface by using alginate.

Besides, it is well established that the peritoneum exploits a reduced immune response, which makes it a preferential transplantation site.[25] This finding can elucidate the decreased fibrotic overgrowth in Figure 6C in contrast to the kidney capsule (Figure 6B).

Summary and Outlook. The results led to the conclusion that particle size, application form, or implantation site influences strongly the immune reaction of the body to an alien system. In light of these observations, a general

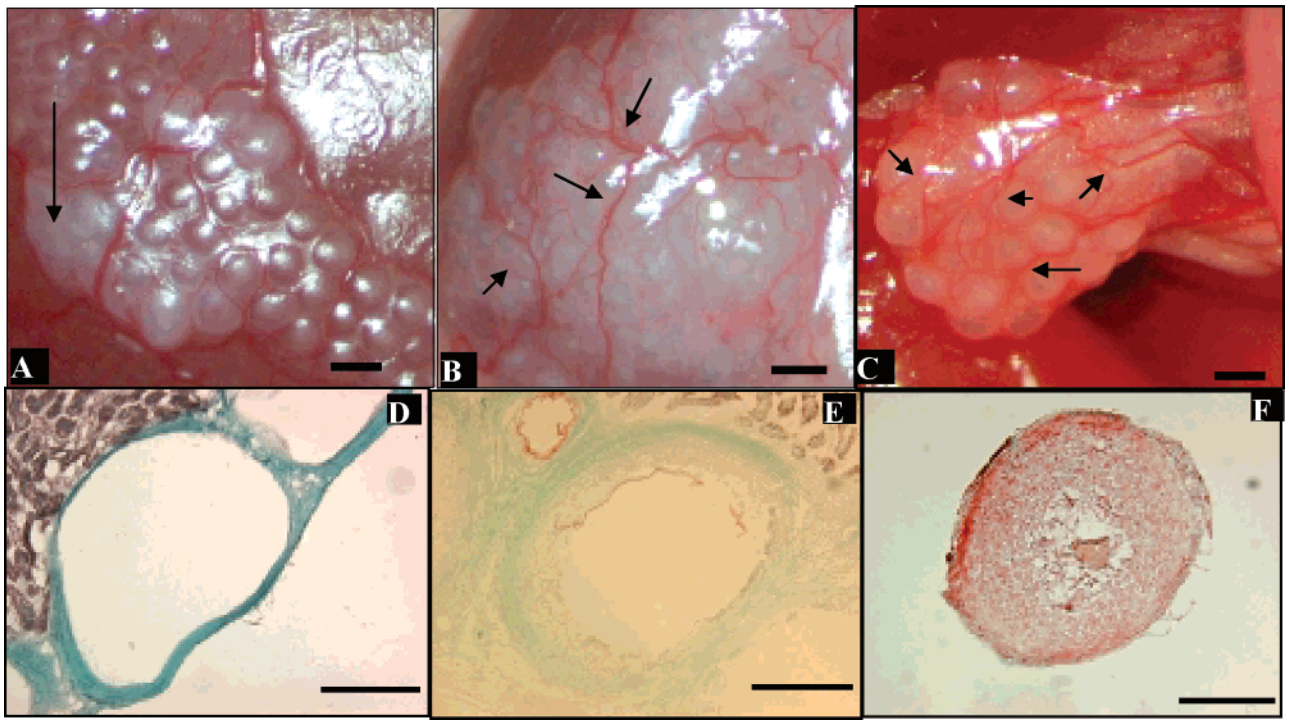

Figure 6. (A−C) Pictures of the implantation sites in a Lewis rat 3 weeks after implantation of alginate beads. The scale bars in panels A−C indicate 500 μm. (A) Uncoated beads underneath the right kidney capsule. The arrow points to the small fibrotic area. (B) PAH/PSS/PAH coated beads underneath the left kidney capsule. The arrows mark the new grown vessels and capillaries. (C) PAH/PSS/PAH coated beads in the peritoneum near the liver. The arrows mark the new grown vessels and capillaries. (D−F) Microscopic images of tissue slices stained with the Masson−Goldner staining. The collagen of the fibrotic region appears bluish-green. (D) Related tissue of the right kidney visualized in panel A. (E) Tissue of the left kidney (see panel B). (F) The connected tissue to the coated beads in the peritoneum (see panel C). The scale bars in panels D−F indicate 200 μm.

statement about the cytotoxicity of a polyelectrolyte is not possible. Moreover, the use of a model system to investigate reactions to polymers remains mainly artificial.

Methods. Gold Core Preparation. The preparation of the monodispersed nanometer-sized gold particles follows the protocol of Turkevich et al.[26] Briefly, 10 mg of $HAuCl_4$ (Aldrich; Milan, Italy) was solved in 100 mL of Milli-Q grade water and boiled under reflux, and then 3.5 mL of a 1% sodium citrate tribasic dihydrate (Aldrich) solution was rapidly added via a syringe to the boiling yellowish solution. After 5 min the color changed to deep red. After boiling for 20 min, the solution was cooled down to room temperature. The particles were found to be stable without remarkable aggregation for 1 month in the dark and in the presence of citrate. The size of the gold nanoparticles was determined from the analysis of 20 particles obtained by TEM (transmission electron microscopy) images with a diameter of 15 $\pm$ 2 nm. Light scattering measurements revealed two main particle sizes. One of approximately 29 nm is presumably the size of single nanogold particles in a shell of citrate ions and water. The size of approximately 200 nm is related to a small quantity of aggregates.

Encapsulation of Nanogold. For the encapsulation of nanogold particles we used the method formerly described by Schneider and Decher[27] with few modifications. In the present study the polyanion PSS (MW 4.3 kDa; Fluka, Steinheim, Germany) was solved with 10 mg/mL concentration in 0.01 M NaCl while the PAH (MW 15 kDa; Aldrich) covalently labeled with FITC (fluoresceine isothiocyanate, λ_{exc} = 488 nm; Fluka) was used in pure water with a concentration of 4 mg/mL like received after dialysis. One milliliter of the citrate-stabilized nanogold solution was added dropwise to 200 μL of the PSS solution. After incubation for 20 min in the dark, the solution was centrifuged for 10 min at 19000*g* with a table centrifuge (Poly Labo, USA). The gel-like deep red pellet was resuspended and washed twice with pure water. Prior to the next layer deposition the coated gold was stored in pure water for 2 h. Then the next polyelectrolyte layer was deposited by adding the gold to 500 μL of the PAH solution. Again, incubation was carried out in the dark for 20 min, followed by centrifugation, washing steps, and storage in water. The maximum number of layers deposited for the presented work was five layers. The deposition was proved by TEM imaging (Figure 5) for up to four layers as well as with the determination of the zeta potential for PSS as first layers as well as for three layers starting with PAH (Figure 7).

Both gold populations detected with light scattering have also different surface charges and can be distinguished by means of zeta potential of coated and uncoated particles (Figure 7). In addition to the results of Schneider and Decher[27] we showed that the encapsulation procedure could be started with PSS instead of PAH as first layer. The quality of the preparation and possible aggregation was followed by the surface plasmon spectrum of the gold solution.

Zeta Potential. The zeta potential measurements were performed with the Malvern Zetasizer Nano-ZS (Worces-

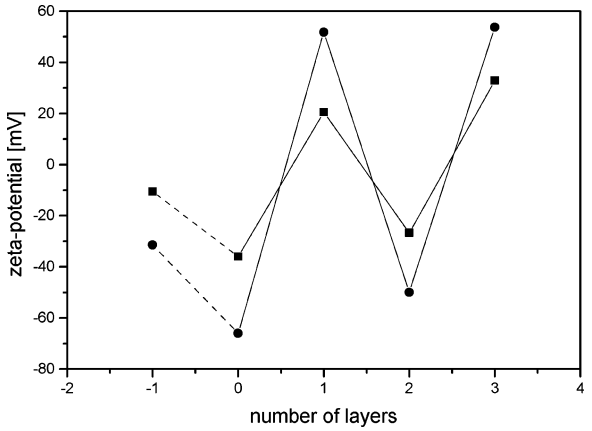

Figure 7. Zeta-potential measurement of the surface charge on coated nanogold. The lines are intended to lead the eye. The dashed line connects the results for the results for PSS as first layer. The solid line indicates the results for the surface charge after deposition of PAH, then PSS, and again PAH. The two values are due to two sizes identified by static light scattering.

tershire, U.K.) and specific electrophoresis cuvettes with an approximately volume of 1 mL at 25 °C. The value of the uncoated nanogold was determined for the untreated nanogold/citrate stock solution. The coated particles were measured in water.

Amorphous Calcium Carbonate Preparation. The preparation of amorphous calcium carbonate was a variation of the method described by Sukhorukov.[28] A sodium carbonate solution (1.08 g/40 mL) was rapidly mixed with calcium chloride (1.48 g) and magnesium chloride (0.2 g) solved in 40 mL of Milli-Q grade water in an ultrasound bath. The chemicals ($CaCl_2 \cdot 2H_2O$, $MgCl_2 \cdot 6H_2O$, Na_2CO_3) for calcium carbonate crystallization were acquired by Fluka (Milan, Italy). Immediately after the addition, the suspension was centrifuged at 2500 rpm for 2 min and twice washed with Milli-Q- grade water. To preserve the amorphous form, it is necessary to dry the material for 1 h at 55 °C. The encapsulation protocol was described in detail elsewhere.[29] Amorphous carbonate was coated with six (outermost coating, PSS (polystyrenesulfonate sodium salt), MW 70 kDa, Aldrich) or seven (outermost coating, PAH (polyallylamine hydrochloride), MW 15 kDa, or PDADMAC (polydiallyldimethylammonium chloride), 240 kDa, both from Aldrich) layers for the cytotoxicity study.

Electric Cell−Substrate Impedance Sensing (ECIS) and Transendothelial Electric Resistance (TEER). The isolation and cultivation protocol for PBCEC is described in detail elsewhere.[30] The final medium, in which the experiments were performed, was serum-free and doped with hydrocortisone. Also for the TEER measurements the protocol of Franke et al.[30] was exactly followed.

The ECIS method is described in detail by Wegener et al.[31] With this method it is possible to distinguish the resistance fraction due to cell−cell contacts from those due to cell−substrate interactions. Briefly, for the measurements the cells were cultivated directly on the gold electrode and the resistance of the cells to an alternating current is measured. The gold electrode (Applied BioPhysics Inc., Troy, NY) consists of eight individual wells with an area of 0.9 cm^2 and a volume of 400 μL. For the continuous wave technique, alternating current was chosen to work with low amplitudes of 0.02 V. Each well contains 10 working electrodes with an area of 5×10^{-4} cm^2 as well as a counter electrode with an area of 0.15 cm^2. The experiments were performed at 37 °C and 5% CO_2 (v/v) in an incubator.

Cytotoxicity Test. 1. In Vitro Experiments on PBCEC. For the cytotoxicity experiments the PBCECs were grown to a confluent cell monolayer. Prior to addition of the PAH solutions as well as the uncoated calcium carbonate particles, the amount of dead cells were determined.

The fluorescent dyes for the live/dead staining, calcein AM and ethidium homodimer (both from Molecular Probes, Eugene, OR) were solved in a modified phosphate-buffered saline (PBS) buffer (0.5 mM $MgCl_2$, 0.9 mM $CaCl_2$, 140 mM NaCl, 2.7 mM KCl, 8.1 mM Na_2HPO_4, 1.5 mM KH_2PO_4) to a concentration of 2 μM for calcein and 4 μM for ethidium homodimer. Then 100 μL of the calcein solution and 100 μL of the ethidium were added to the cell medium, the cells were incubated for 45 min, and the staining was visualized by fluorescence microscopy.

To test the toxicity of $CaCO_3$, 20 mg was suspended in 200 μL of cell medium which was removed from the culture medium and afterward replaced. For PAH 50, 100, and 200 μL of the cell culture medium were exchanged with the same volume of polycation solution (concentration of 2 mg/mL). The phenol red pH indicator changed colors from yellow to red indicating a diminution of the pH value.

After incubation for 10 min, the supernatant of the cells was replaced by fresh medium. In the case of crystals, it was necessary to wash the sample three times with PBS buffer to remove the crystals from the cell layer before adding again medium. Then the staining was carried out, and the fluorescence images were acquired.

Cytotoxicity Test. 2. In Vivo Experiments in Rats. First empty barium−alginate microbeads were produced by pushing 2% solution of highly purified alginate (Pronova UP MVG, NovaMatrix, Oslo, Norway) through a 0.8 mm inner nozzle; changing the airflow in the outer nozzle regulated the size of the microbeads. All microbeads were gelled in 30 mL of gelling solution per 1 mL of alginate (30 mM $BaCl_2$ for 4 min). The bead size was 300−600 μm.

Adult male Lewis rats, body weight 260−300 mg, were used for biocompatibility studies. The animals were kept in a small-animal house and allowed free access to food and water. The implantation of the microbeads was performed under general anesthesia: 1−3% Isofluran (Baxter, Munich, Germany) and 100% oxygen. Immediately before implantation the microbeads were washed with 0.9% NaCl and transferred into the microliter syringe. The alginate beads coated with PAH/PSS/PAH were transplanted beneath the capsule of the left kidney. As controls, the alginate microbeads without coating were implanted under the capsule of the right kidney of the same animal. The peritoneal cavity was additionally used as the implantation site for both types of beads. Postsurgical analgesia was maintained by subcutaneous injection of Tramal (Grünenthal, Stolberg, Germany).

The macroscopic examination and histological studies were performed 30 days after implantation. All principles of laboratory care were followed. The study was approved by the local Animal Ethics Committee.

Acknowledgment. M.C. thanks DAAD (Deutscher Akademischer Austauschdienst, Germany), Professor Wierich, and Dr. Grave for financial support. Further, the authors thank Dott.ssa P. Rubini and Dott.ssa P. Luzzi as well as P.D. Dr. J. Wegener and Dr. B. Reiss, Institute of Biochemistry, University of Münster, for the technical support.

References

(1) Lim, F.; Sun, A. M.; Microencapsulated islets as bioartificial endocrine pancreas. *Science* **1980**, *210*, 908−910.
(2) Davis, M. W.; Vacanti, J. P.; Toward development of an implantable tissue engineered liver. *Biomaterials* **1996**, *17*, 365−372.
(3) Soon-Shiong, P.; et al. Insulin independence in a type 1 diabetic patient after encapsulated islet transplantation. *Lancet* **1994**, *343*, 950−951.
(4) De Vos, P.; Marchetti, P. Encapsulation of pancreatic islets for transplantation in diabetes: the untouchable islets. *Trends Mol. Med.* **2002**, *8*, 363−366.
(5) De Groot, M.; et al. Microcapsules and their ability to protect islets against cytokine-mediated dysfunction. *Transplant. Proc*. **2001**, *33*, 1711−1712.
(6) Gaumann, A.; et al.; Xenotransplantation of parathyroids in rats using barium-alginate and polyacrylic acid multilayer microcapsules. *Exp. Toxicol. Pathol.* **2001**, *53*, 35−43.
(7) Takeshi A.; et al. Intrasplenic Transplantation of Encapsulated Hepatocytes Decreases Mortality and Improves Liver Functions in Fulminant Hepatic Failure from 90% Partial Hepatectomy in Rats. *Transplantation* **2005**, *79*, 783−790.
(8) Antipov, A. A.; Sukhorukov, G. B. Polyelectrolyte multilayer capsules as vehicles with tunable permeability. *Adv. Colloid Interface Sci*. **2004**, *111*, 49−61.
(9) Chluba, J.; et al. Peptide hormone covalently bound to polyelectrolytes and embedded into multilayer architectures conserving full biological activity. *Biomacromolecules* **2001**, *2*, 800−805.
(10) Decher, G. Fuzzy nanoassemblies: Toward layered polymeric multicomposites. *Science* **1997**, *277*, 1232−1237.
(11) Möhwald, H. From Langmuir monolayers to Nanocapsules. *Colloids Surf., A* **2000**, *171*, 25−31.
(12) Diaspro, A.; Silvano, D.; Krol, S.; Cavalleri, O.; Gliozzi, A. Single living cell encapsulation in nano-organized polyelectrolyte shells. *Langmuir* **2002**, *18*, 5047−5050.
(13) Krol, S.; et al. Nanocapsules: Coating for Living Cells. *IEEE Trans. Nanobiosci.* **2004**, *3*, 32−38.
(14) Boussif, O.; et al. Synthesis of Polyallylamine Derivatives and Their Use as Gene Transfer Vectors in Vitro. *Bioconjugate Chem*. **1999**, *10*, 877−883.
(15) De Rosa, M.; et al. Cationic polyelectrolyte hydrogel fosters fibroblast spreading, proliferation, and extracellular matrix production: Implications for tissue engineering. *J. Cell. Physiol.* **2004**, *198*, 133−143.
(16) Goodman, C. M.; McCusker, C. D.; Yilmaz, T.; Rotello, V. M. Toxicity of Gold Nanoparticles Functionalized with Cationic and Anionic Side Chains. *Bioconjugate Chem*. **2004**, *15*, 897−900.
(17) Yin, H.; Too, H. P.; Chow, G. M. The effects of particle size and surface coating on the cytotoxicity of nickel ferrite. *Biomaterials* **2005**, *26*, 5818−5826.
(18) Liu, W. K.; Tam, J. S. K.; Wong, M. H. Size dependent cytotoxicity of fly ash particles. *Environ. Int.* **1988**, *14*, 473−477.
(19) Rodrigo, A. M.; et al. Influence of particle size in the effect of polyethylene on human osteoblastic cells. *Biomaterials* **2001**, *22*, 755−762.
(20) Bickel, U.; Yoshikawa, T.; Pardridge, W. M. Delivery of peptides and proteins through the blood-brain barrier. *Adv. Drug Delivery Rev.* **2001**, *46*, 247−279.
(21) Zhu, Y.; Gao, C.; He, T.; Liu, X.; Shen, J. Layer-by-Layer Assembly To Modify Poly(L-lactic acid) Surface toward Improving Its Cytocompatibility to Human Endothelial Cells. *Biomacromolecules* **2003**, *4*, 446−452.
(22) Klueh, U.; Dorsky, D. I.; Kreutzer, D. L. Enhancement of implantable glucose sensor function in vivo using gene transfer-induced neovascularization. *Biomaterials* **2005**, *26*, 1155−1163.
(23) Amirpour, M. L.; Ghosh, P.; Lackowski, W. M.; Crooks, R. M.; Pishko, M. V. Mammalian cell cultures on micropatterned surfaces of weak acid, polyelectrolyte hyperbranched thin films on gold. *Anal. Chem*. **2001**, *73*, 1560−1566.
(24) Elbert, D. L.; Herbert, C. B.; Hubbell, J. A. Thin polymer layers formed by polyelectrolyte multilayer techniques on biological surfaces. *Langmuir* **1999**, *15*, 5355−5362.
(25) Soon-Shiong, P.; et al. Long-term reversal of diabetes by the injection of immunoprotected islets. *Proc. Natl. Acad. Sci. U.S.A.* **1993**, *90*, 5843−5847.
(26) Turkevich, J.; Stevenson, P. C.; Hillier, J. A study of the nucleation and growth processes in the synthesis of colloidal gold. *Discuss. Faraday Soc*. **1951**, *11*, 55−75.
(27) Schneider, G.; Decher, G. From Functional Core/Shell Nanoparticles Prepared via Layer-by-Layer Deposition to Empty Nanospheres. *Nano Lett.* **2004**, *4*, 1833−1839.
(28) Antipov, A. A., et al.; Carbonate microparticles for hollow polyelectrolyte capsules fabrication. *Colloids Surf., A* **2003**, *224*, 175−183.
(29) Silvano, D.; Krol, S.; Cavalleri, O.; Diaspro, A.; Gliozzi, A. Polyelectrolyte multilayer nanocapsules derived from CdCO3 templates analyzed by means of confocal laser scanning microscopy. *Microsc. Res. Tech*. **2002**, *59*, 536−541.
(30) Franke, H.; Galla, H.-J.; Beuckmann, C. Primary cultures of brain microvessel endothelial cells: A valid and flexible model to study drug transport through the blood-brain-barrier in vitro. *Brain Res. Protoc.* **2000**, *5*, 248−256.
(31) Wegener, J.; Keese, C. R.; Giaever, I. Electric Cell-substrate impedance sensing (ECIS) as a noninvasive means to monitor the kinetics of cell spreading to artificial surfaces. *Exp. Cell Res.* **2000**, *259*, 158−166.

NL0521219